CRYOMODULE PROTECTION FOR ARIEL E-LINAC

Z. Yao#, R.E. Laxdal, W.R. Rawnsley, V. Zvyagintsev, TRIUMF, Vancouver, B.C., Canada

Abstract

The e-Linac cryomodules require high RF power, cryogenics, ultra-high vacuum, and precise mechanical adjustment. They require protection against of failures, like quench in the cavity, bad vacuum or multipacting in power couplers, low liquid helium level or high temperatures. The protection unit should stop RF power in the cryomodule in case of the listed failures. An Interlock Box is developed to implement protection function for the cryomodule. The paper will describe the design of Interlock Box for e-Linac cryomodule protection. As quench protection required, quench evolution analysis with RF transient analysis is investigated. The details of quench detection for e-Linac will also be reported.

INTRODUCTION

The ARIEL e-Linac is a CW 10mA 50MeV electron LINAC [1]. It consists of one injector cryomodule with one 9-cell cavity and two accelerator cryomodules with two 9-cell cavities each. The nominal operating accelerating gradient of the superconducting cavity is 10MV/m at the power dissipation on cavity wall of 10W [2]. As the high intensity beam loading, each cavity requires 100kW RF power. Two 300kW klystrons provide RF power for injector and one accelerator cryomodule. Each cavity has two 50kW CPI RF power couplers.

In general, cryomodule is a cryo-vacuum chamber. Vacuum leak, local high temperature and low helium level should be prevented during operation.

The RF power couplers were conditioned up to 20kW [3] in CW mode with traveling wave on the room temperature power coupler test stand. They to be conditioned to operational power level of equivalent 50kW in-situ. Couplers require protection to prevent damage in case of multipacting, discharge or vacuum activity.

The specification of cavity quality factor is 1×10^{10} at operational gradient of 10MV/m. Due to the 100kW beam power requirement, the external quality factor of pair couplers is 10^6. In case of cavity quench, part of the superconducting cavity wall switches to normal conducting state, and decreases cavity Q_0. More RF power will dissipate on cavity wall, and cryogenic system loading will increase beyond its capability. A reliable fast trip is required to protect cryogenic system due to SRF cavity quench and high beam loading.

To protect cryomodule and cryogenic system in operation, fast hardware interlock boxes are designed and produced for ARIEL e-Linac. This paper will discuss the theoretical analysis of cavity quench detection for ARIEL specification, and the design of cryomodule interlock box.

#zyyao@triumf.ca

QUENCH DETECTION ANALYSIS

Cavity quench in cryomodule can be detected from changes of helium pressure, liquid level, cavity temperature. The limitation of these measurements is a long response time.

When the cavity quenches, the ‘defect’ area switches to normal conducting state. More RF power is dissipated, and the ‘defect’ is growing and increasing RF power dissipation. The cavity Q_0 decreases from operation specification 10^{10} to close to coupler Q_{ext} 10^6. The Q_0 of a quenched cavity is assumed to be 10^6. RF power loss on cavity inner surface is 45kW for full beam loading limit, and 100kW for no beam loading limit. The ARIEL e-Linac cryogenic system capability is 100J/s per cavity for RF power consumption. To protect cryogenic system, RF power to the cavity should be stopped in 1ms after cavity quench.

In CW operation, cavities are controlled by feedback system. TRIUMF’s LLRF feedback system has a typical cycle time of 1ms. For longer periods than 1ms after cavity quench, LLRF will increase amplitude drive for RF forward power to compensate the reduction of cavity accelerating field. The positive feedback effect limits quench detection and protection in 1ms.

As the fast response requirement, RF signal is proposed for quench detection. Quench evolution and RF transient analyses are developed.

Cavity Quench Evolution Analysis

A quench evolution model has been developed based on COMSOL Multiphysics model, shown in Fig. 1. The upper boundary of each model is helium surface, and lower one is RF surface. The left side is symmetry axis, where a defect exists on RF surface, and right side is unlimited boundary. The model simulates growth rate of the normal conducting zone during a cavity quench.

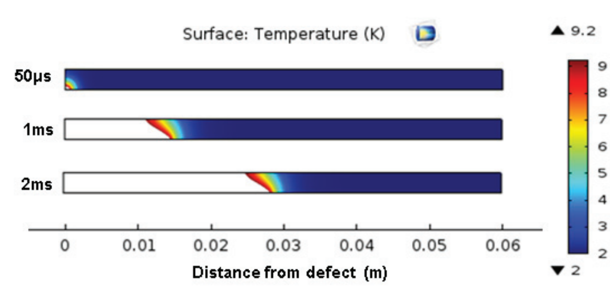

Figure 1: 2D axial symmetry quench evolution model in COMSOL Multiphysics. The plots show temperature distribution in cavity wall during quench at 50µs, 1ms and 2ms. White color shows normal conducting zone.

The simulation result for radius evolution of the normal conducting zone is 14.1mm/ms with e-LINAC specification. Assume that cavity quench is happening at

ISBN 978-3-95450-178-6

T_{quench}, the radius of normal conducting zone r is

$$r = 14065 \cdot (t - T_{quench})$$

Normal zone area is

$$S_n = \pi r^2$$

The quenched cavity quality factor $Q_0{}'$

$$Q_0{}' = \frac{G}{R_n \frac{S_n}{S_{total}} + R_s \left(1 - \frac{S_n}{S_{total}}\right)}$$

which is shown in Fig. 2.

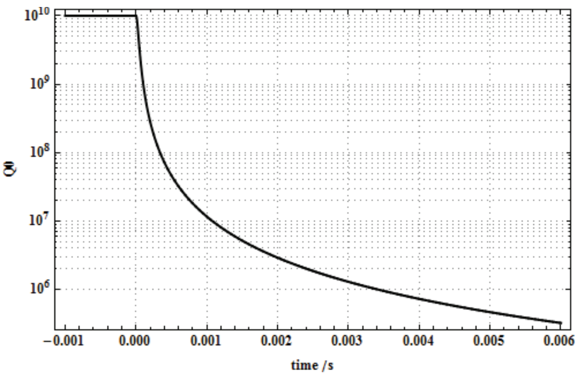

Figure 2: Cavity Q_0 evolution during cavity quench. Quench happens at 0s.

RF Transient Analysis

RF forward, reverse power and cavity pickup signal are under measurements. If cavity quenches, the coupling condition is changed, and RF power and cavity voltage follow changing. The transient is studied to predictRF signals change during cavity quench. In addition, the different beam loading conditions, such as pulse or CW beam, and different current intensity, are analysis for different operation regime.

Based on the equivalent circuit analysis, the differential equation of cavity voltage with cavity detuning and beam loading is

$$\ddot{V_c} + 2\left(\omega_{\frac{1}{2}} + i\omega\right)\dot{V_c} + [2\omega\left(\delta\omega + i\omega_{\frac{1}{2}}\right) + \delta\omega^2]V_c = 2r_L\omega_{\frac{1}{2}}(\dot{I} + i\omega I)$$

where Vc is cavity voltage, I is sum current including equivalent RF current and beam current, $\delta\omega$ is the differential frequency of detuned cavity, $\omega_{\frac{1}{2}}$ is cavity bandwidth and $r_L = \frac{R_a}{Q_0} \cdot \frac{Q_L}{2}$. Mathematica code is written with finite difference method [4] to solve equations as

$$V_{cr,t+\Delta t} = V_{cr,t} + (K_{11,t} + K_{21,t})/2$$
$$V_{ci,t+\Delta t} = V_{ci,t} + (K_{12,t} + K_{22,t})/2$$

where

$$K_{11,t} = \Delta t(-\omega_{\frac{1}{2}}V_{cr,t} - \delta\omega V_{ci,t} + r_L\omega_{\frac{1}{2}}I_{r,t})$$
$$K_{12,t} = \Delta t(\delta\omega V_{cr,t} - \omega_{\frac{1}{2}}V_{ci,t} + r_L\omega_{\frac{1}{2}}I_{i,t})$$
$$K_{21,t} = \Delta t[-\omega_{\frac{1}{2}}(V_{cr,t} + K_{11,t}) - \delta\omega(V_{ci,t} + K_{12,t}) + r_L\omega_{\frac{1}{2}}I_{r,t}]$$
$$K_{22,t} = \Delta t[\delta\omega(V_{cr,t} + K_{11,t}) - \omega_{\frac{1}{2}}(V_{ci,t} + K_{12,t}) + r_L\omega_{\frac{1}{2}}I_{i,t}]$$

With predefined forward power, beam loading and previous quenched cavity Q_0 evolution conditions, the simulation code predicts transient variations of loaded Q, cavity voltage amplitude and phase, and RF reverse power. An example of quench at 10MV/m operation gradient with CW 100kW beam loading is shown in Fig. 3. The measurable changes for accelerating gradient and forward power in 1ms during cavity quench can be figured out.

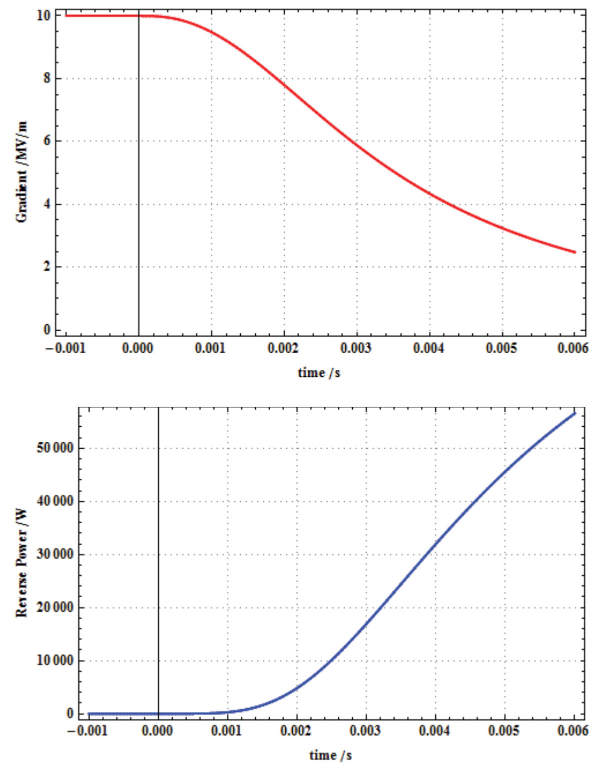

Figure 3: Cavity accelerating gradient (top) and RF reverse power (bottom) variation during cavity quench happens at 0s.

ARIEL e-Linac Quench Detection

With tools of quench evolution and RF transient analyses, quench detection has been studied for pulse conditioning, open loop CW RF and close loop operation conditions.

For RF pulse conditioning regime the cavity is in open loop without beam loading. As an ideal superconducting cavity, 100kW forward power drives cavity gradient to 20MV/m and the cavity power loss of 40W with $Q_{ext}=10^6$. The filling time is 0.1ms. If cavity quenches, Q_0 drops to 10^6, which is match condition, in about 0.8ms. When couplers match quenched cavity, all RF power will be consumed on cavity wall and loaded to cryogenic system. In order to limit heat dissipation to 100J/s, the RF pulses width should be limited to 1ms assuming a RF repetition rate of 1Hz. In case of RF pulse conditioning mode no quench detection is required if the duty factor is limited.

ISBN 978-3-95450-178-6

For close loop operation, pulse and CW beams with different current intensities are analyzed. When RF is in close loop, unless cavity quenches, the cavity gradient is maintained at 10MV/m by LLRF. Fig. 3 shows the gradient variation during cavity quench with CW beam loading, while Fig. 4 shows that with pulse beam loading. A summary diagram for different beam loadings conditions, pulse beam duty factors, and coupling factors is shown in Fig. 5. CW beam loading is represented by 100% duty factor.

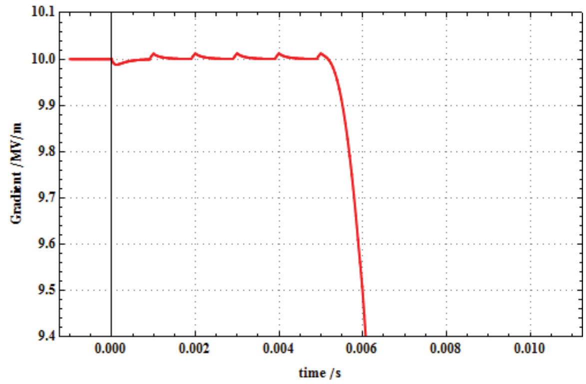

Figure 4: Cavity accelerating gradient variation due to transient beam loading and cavity quench happens at 5ms.

The close loop transient analysis shows cavity gradient drops at least 5% in 1ms after cavity quench happens. Comparing to pulse beam load transient, the gradient variation is 20 times more, which is sufficient large to avoid noise trigger of quench detector.

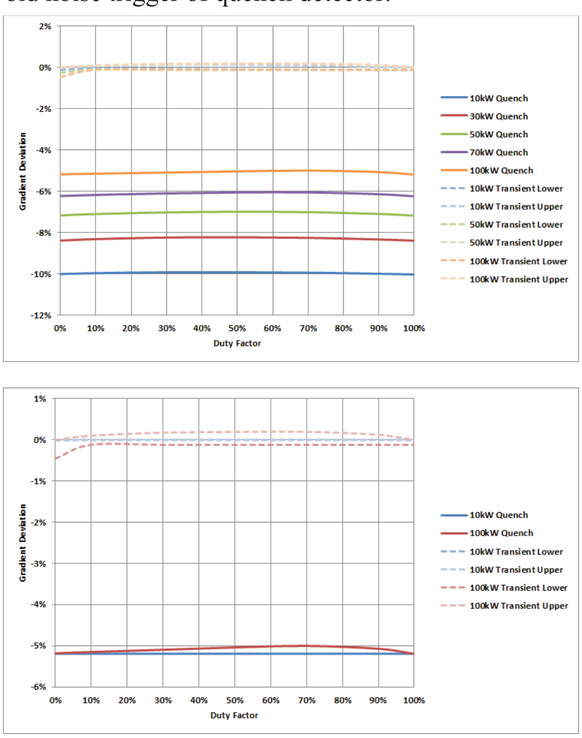

Figure 5: Comparison of cavity gradient changes due to beam transient and cavity quench (1ms) for different beam loading conditions with the optimized Q_{ext} (top) and $Q_{ext}=10^6$ (bottom).

In open loop condition without beam loading, and cavity gradient is manually changed, or changed by automatic sequence of LLRF program. The cavity gradient cannot be used as a quench detection indicator. RF reverse power is taken in to account. When cavity quenches, it consumes much more RF power, and such a way RF reverse power decreases. But when RF is turned on or forward power is increased, transient reverse power drops too, which will be a false trigger signal. Hence, the gradient changes should be limited to 1MV/m each step, and quench detector can be used when the cavity gradient is higher than 5MV/m, which is a relaxed level for cavity quench. To get a uniform reference power level, the ratio of reverse power and forward power is used as a threshold to detect a cavity quench, as a change of -15dB in 3ms, shown in Fig. 6.

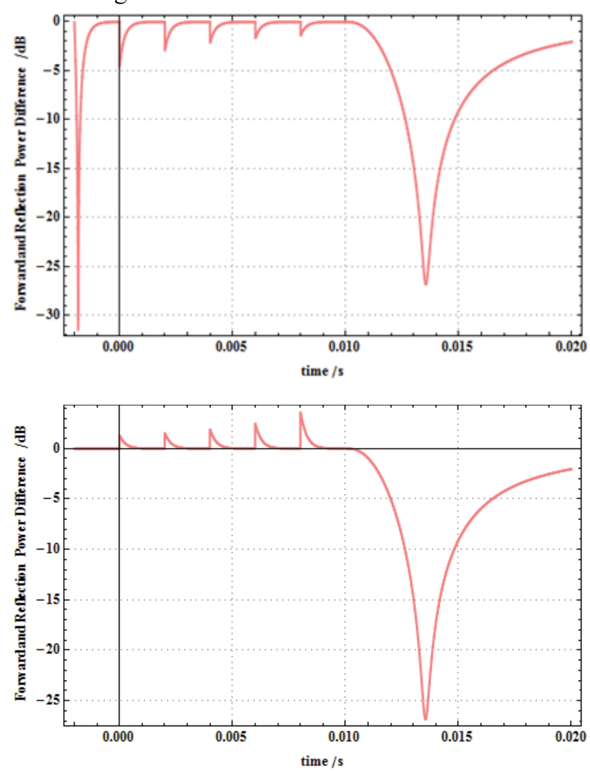

Figure 6: The ratio of reverse power and forward power in dB scale during RF transient and cavity quench. The increasing gradient case is shown in top plot, and decreasing case in bottom.

CRYOMODULE INTERLOCK BOX

The cryomodule interlock box is a hardware protection system designed for ARIEL e-Linac fast interlock. In case of cavity quench, multipacting in power couplers, vacuum spike, low liquid helium level, or high temperature, the interlock box cuts off RF drive signal from LLRF to klystron, to protect cryomodule and cryogenic system. The main parts of the interlock box are FPGA, which processes trip signals and provide protection latching, and RF switcher, that controls RF drive signal through or not.

ISBN 978-3-95450-178-6

One interlock box has capability to protect two cavities or one cryomodule. The block schematic of the interlock box is shown in Fig. 7. The monitoring signals are shown in Fig. 8. Each interlock box module has 25 input signals, including vacuum, RF, PMT, control, and PLC signals.

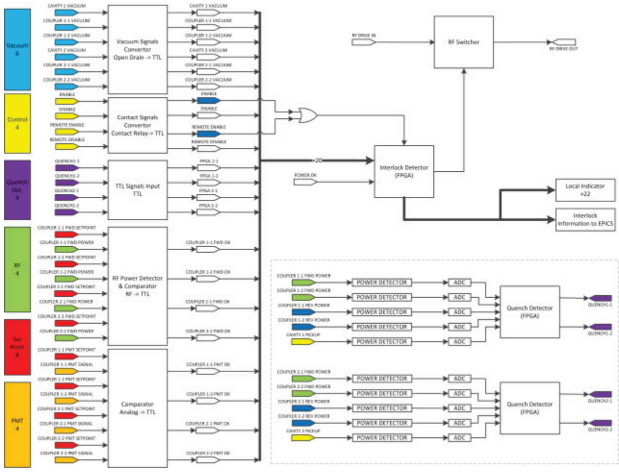

Figure 7: General schematic of cryomodule interlock box.

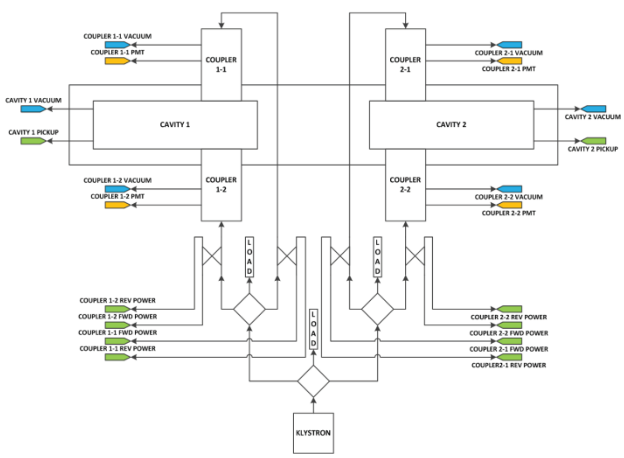

Figure 8: Monitoring signals from accelerator cryomodule.

The interlock box is mounted on standard 19” rack. Control switches, LED indicators, trip level adjustment ports, and test points are laid on front panel. The rare panel consists of signals input and output connectors, power supply, and fuses. Panels are shown in Fig. 9.

Coupler and cavity vacuum are measured by Agilent UHV-24 ion gauge, and read by Varian XGS-600 gauge controller. The vacuum trip level can be set in controller, and trip signal outputs from Set-Point connector by an open collector with ground reference. 12V DC voltage is applied on Set-Point output. If pressure is higher than setpoint, open collector is in open state, and interlock box receives a low logic signal, then trips RF.

RF signals are coupled from directional coupler on transmission line, and converted to analog signal by Mini-circuit ZX47-40+ negative RF power detectors. The linear dynamic range is 60dB, and output voltage range is 0.5V to 2.1V. The signals are processed by power limit comparator or quench detector. A low logic signal can trip RF drive.

Coupler multipacting or discharge is monitored by coupler vacuum and photo signal. H10722-01 type photo sensors, which consist of metal package PMT, are installed on glass windows close to warm windows of power couplers. Power supply, trip level setpoint, and comparator are integrated in interlock box. The output logic is same as RF signals.

EPICS communicates with interlock box through PLC. It reads latch signal for trip information, remotely controls and resets, and sends slow trip signal, which includes liquid helium level, cryomodule temperatures, cooling system status, and other potential trip signal.

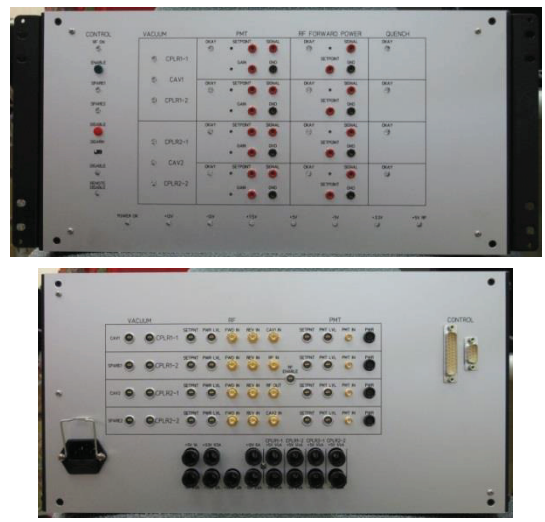

Figure 9: Front (top) and rare (bottom) panels of interlock box.

The interlock box is a developing module. It has test points for input signals and adjustable trip level. FPGA development board and spare input channels offer capability of upgrade.

CONCLUSION

To protect cryomodule and cryogenic systema cryomodule interlock box for ARIEL e-Linac has been designed, manufactured and successfully used for commissioning of two cryomodules.. During the tests it shown fast and reliable operation. As quench detection requirement, quench evolution and RF transient with ARIEL e-Linac specification are analyzed. The hardware development of quench detector and interlock box development and upgrade are in progress.

REFERENCES

[1] V. Zvyaginstev et al., Commissioning of the SRF Linac for ARIEL, this conference, SRF ’15, histler, Canada, TUAA02.
[2] P. Kolb et al., 1.3 GHz Cavity Test Program for ARIEL, this conference, SRF ’15, MOPB089.
[3] Y. Ma et al., High Power Coupler Test for Ariel SC Cavities, this conference, SRF ’15, THPB103.
[4] S. Kim, M. Doleans, Principles of Superconducting Linear Accelerators, USPAS, 2013.

ISBN 978-3-95450-178-6